AD-A053 461 NAVAL OCEAN SYSTEMS CENTER SAN DIEGO CA F/G 9/4
ADAPTIVE ENHANCEMENT OF MULTIPLE SINUSOIDS IN UNCORRELATED NOIS--ETC(U)
OCT 77 J R ZEIDLER, E H SATORIUS

UNCLASSIFIED NOSC/TR-193 NL

1 OF 1
ADA
053461

END
DATE
FILMED
6-78
DDC

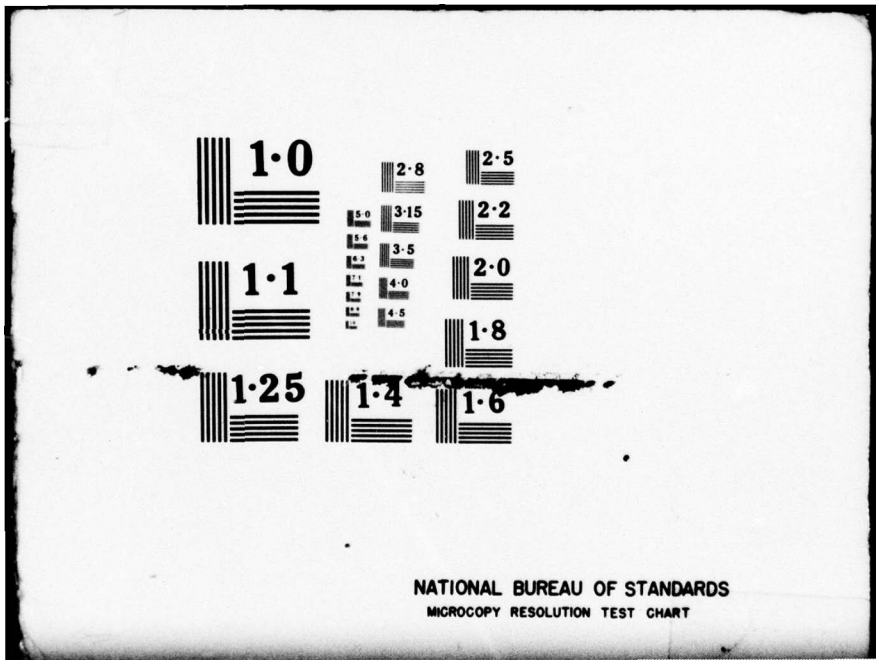
1·0
1·1
1·25
1·4
1·6
1·8
2·0
2·2
2·5
2·8
3·15
3·5
4·0
4·5
NATIONAL BUREAU OF STANDARDS
MICROCOPY RESOLUTION TEST CHART

(12)

NOSC

NOSC / TR 193

NOSC / TR 193

Technical Report 193

ADAPTIVE ENHANCEMENT OF MULTIPLE SINUSOIDS IN UNCORRELATED NOISE

JR Zeidler
EH Satorius
DM Chabries
HT Wexler

1 October 1977

Final Report: October 1976 — September 1977

Prepared for
NAVAL ELECTRONIC SYSTEMS COMMAND

Approved for public release; distribution unlimited.

NAVAL OCEAN SYSTEMS CENTER
SAN DIEGO, CALIFORNIA 92152

NAVAL OCEAN SYSTEMS CENTER, SAN DIEGO, CA 92152

AN ACTIVITY OF THE NAVAL MATERIAL COMMAND

RR GAVAZZI, CAPT, USN
Commander

HL BLOOD
Technical Director

ADMINISTRATIVE INFORMATION

This report is a preprint of a paper accepted for publication in the IEEE *Transaction on Acoustics, Speech, and Signal Processing.* Copyright 1978 by the Institute of Electrical and Electronics Engineers, Inc.; printed by permission. The work reported was sponsored by the Naval Electronic Systems Command (Code 320) under program element 62711N, task area XF11-121, and performed during fiscal year 1977.

Released by
R. H. HEARN, Head
Electronics Division

Under authority of
D. A. KUNZ, Head
Fleet Engineering Department

ACKNOWLEDGMENTS

The authors wish to express their thanks to P. Reeves, J. McCool, S. Alexander and R. Hearn of the Naval Ocean Systems Center; J. Treichler and B. Widrow of Stanford University; and L. Griffiths of the University of Colorado for their many helpful comments throughout the course of this work. The authors are also indebted to R. Fraser of the Naval Ocean Systems Center for assistance in preparing this paper.

UNCLASSIFIED

SECURITY CLASSIFICATION OF THIS PAGE (When Data Entered)

REPORT DOCUMENTATION PAGE	READ INSTRUCTIONS BEFORE COMPLETING FORM
1. REPORT NUMBER: NOSC/TR-193 (14)	2. GOVT ACCESSION NO. / 3. RECIPIENT'S CATALOG NUMBER
4. TITLE (and Subtitle): Adaptive Enhancement of Multiple Sinusoids in Uncorrelated Noise (6)	5. TYPE OF REPORT & PERIOD COVERED: Final: 10/76-9/77 / 6. PERFORMING ORG. REPORT NUMBER
7. AUTHOR(s): J. R. Zeidler, E. H. Satorius, D. M. Chabries, H. T. Wexler (10)	8. CONTRACT OR GRANT NUMBER(s): Final rept. Oct 76-Sep 77 (9)
9. PERFORMING ORGANIZATION NAME AND ADDRESS: Naval Ocean Systems Center, San Diego, Calif. 92152	10. PROGRAM ELEMENT, PROJECT, TASK AREA & WORK UNIT NUMBERS: 62711N, F11-121
11. CONTROLLING OFFICE NAME AND ADDRESS: Naval Electronic Systems Command, Washington, D.C.	12. REPORT DATE: 1 Oct 1977 (11) / 13. NUMBER OF PAGES: 33 (12) 37p
14. MONITORING AGENCY NAME & ADDRESS (if different from Controlling Office)	15. SECURITY CLASS. (of this report): Unclassified / 15a. DECLASSIFICATION DOWNGRADING SCHEDULE
16. DISTRIBUTION STATEMENT (of this Report): Approved for public release; distribution unlimited. (16) F11121 (17) XF11121	
17. DISTRIBUTION STATEMENT (of the abstract entered in Block 20, if different from Report)	
18. SUPPLEMENTARY NOTES	
19. KEY WORDS (Continue on reverse side if necessary and identify by block number)	

20. ABSTRACT (Continue on reverse side if necessary and identify by block number)

The steady-state behavior of the adaptive line enhancer (ALE), a new implementation of adaptive filtering that has application in detecting and tracking narrowband signals in broadband noise, is analyzed for a stationary input consisting of multiple sinusoids in white noise. It is shown that the steady-state performance of an L-weight ALE for this case can be modeled by the L X L Wiener-Hopf matrix equation and that this matrix equation can be transformed into a set of 2N coupled linear equations, where N is

DD FORM 1 JAN 73 1473 EDITION OF 1 NOV 65 IS OBSOLETE

UNCLASSIFIED

SECURITY CLASSIFICATION OF THIS PAGE (When Data Entered)

393 159

8

20. Abstract (cont.)

the number of sinusoids. It is also shown that the expected values of the ALE weights in steady state can be written as a sum of sinusoids and that the amplitude of each sinusoid is coupled to that of all other sinusoids by coefficients that approach zero as the number of ALE weights becomes large. The analytical results are compared to experimental results obtained with a hardware implementation of the ALE of variable length (up to 256 weights) and show good agreement. Theoretical expressions for linear predictive spectral estimates are also derived for multiple sinusoids in white noise. Comparisons are made between the magnitude of the discrete Fourier transform of the ALE weights and the linear predictive spectral estimate for two sinusoids in white noise.

CONTENTS

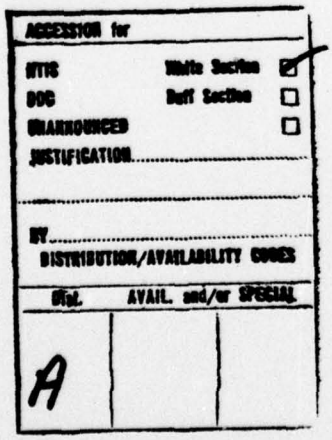

I. INTRODUCTION

A new method of enhancing the detectability of narrowband signals in the presence of broadband noise has recently been introduced [1,2,3]. This method, called "adaptive line enhancement," is based on the Widrow-Hoff least-mean-square (LMS) adaptive algorithm. As shown in Fig. 1, it is implemented with a two-channel processor in which a delayed version of the input data is adaptively filtered and subtracted from the instantaneous input data. The difference between the delayed and instantaneous data serves as the error signal $\epsilon(j)$ for the LMS algorithm, which governs the frequency response of the adaptive filter in such a way that the power of $\epsilon(j)$ is minimized.

Operation of the adaptive line enhancer (ALE) of Fig. 1 can be understood intuitively as follows. The delay causes decorrelation between the noise components of the input data in the two processor channels while introducing a simple phase difference between the sinusoidal components. The adaptive filter responds by forming a transfer function equivalent to that of a narrowband filter centered at the frequency of the sinusoidal components. The noise component of the delayed input is rejected, while the phase difference of the sinusoidal component is readjusted so that they cancel each other at the summing junction, producing a minimum error signal composed of the noise component of the instantaneous input data alone.

Use of the ALE to detect sinusoidal signals in uncorrelated or "white" noise is discussed in [1], [2], and [3].[1] In this application any value Δ of delay can be chosen. The ALE can also be used to detect sinusoidal signals in correlated or "colored" noise [2]. In this case it is often necessary to choose a relatively large value of Δ to insure decorrelation between the noise components in the two processor channels.

The ALE with unit delay ($\Delta = 1$) is identical to the instantaneous frequency tracker of [4].[2] The ALE and instantaneous frequency tracker are further shown in [5] to be forms of adaptive linear prediction filter. A comprehensive treatment of linear prediction filtering techniques is given in [6] and [7]. The LMS algorithm was first applied to the design of an adaptive prediction filter in [14]. A recent hardware implementation of an 8-weight LMS adaptive linear predictor and its application to instantaneous frequency estimation, speech encoding, and other similar problems are discussed in [8].

The advantages of adaptive line enhancing with respect to conventional digital Fourier analysis have been discussed with some controversy in the literature. A comparison in [1], using figures of merit based on output signal-to-noise ratio, indicated that the ALE required less data to achieve a given level of detection performance. This comparison was shown to be in error in [9], and a correction presented in [10] indicated that performance with a given amount of data was equivalent. A definitive comparison based on statistical detection theory, however, has not yet been published. Considering the fundamental

---

[1] Detection is accomplished by digital Fourier analysis of the adaptive filter weights [1,2] or adaptive filter output [3].

[2] In this application a modified maximum entropy spectral estimate is computed from the adaptive filter weights.

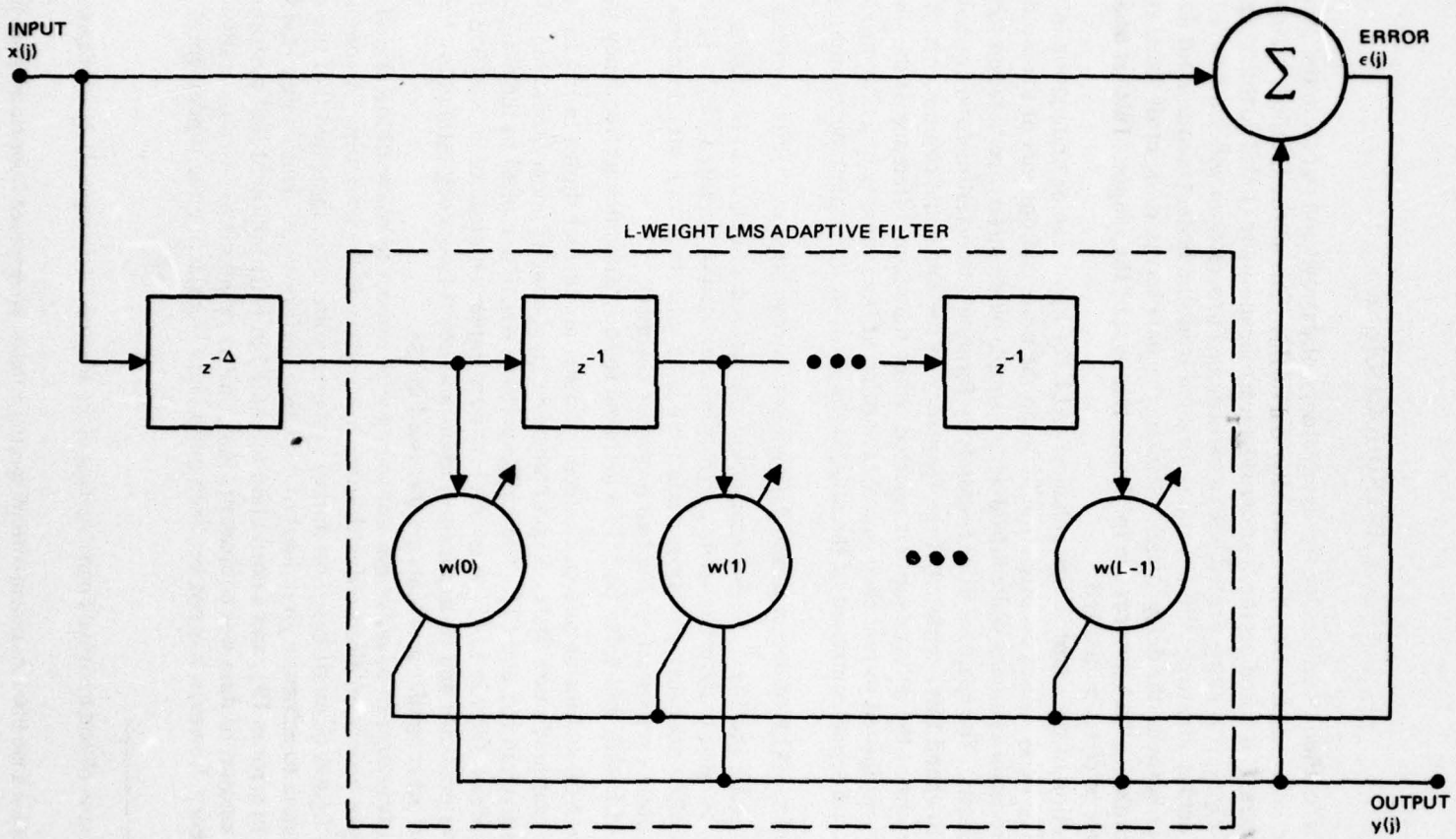

Figure 1. Adaptive line enhancer (ALE).

differences between the two methods it appears likely that each will have advantages in different applications.[3] As suggested in [11], the ALE in many applications is effective over a wide range of input signal and noise parameters with little a priori information. Both [10] and [11] have also emphasized its ability to resolve closely spaced narrowband signals.

Since the ALE is a new type of processor, many questions regarding its performance and advantages remain to be answered. The goal of this paper is to analyze its steady-state behavior with a stationary input consisting of multiple sinusoids in uncorrelated noise. It will be shown, using the method of undetermined coefficients, that the L × L Wiener-Hopf matrix equation describing the steady-state impulse response of an L-weight ALE with arbitrary delay or "prediction distance" Δ may be transformed into a set of 2N coupled linear equations, where N is the number of sinusoids in the ALE input. This set of equations, which decouples as the adaptive filter becomes longer, provides a useful description of the interaction between the sinusoids introduced by the finite length of the filter. The derived impulse responses and transfer functions form an analytical basis for comparing in terms of L and Δ the various techniques of obtaining spectral estimates with the ALE for this class of input signals. These results also offer a means of comparing spectral estimates obtained with adaptive line enhancing and those obtained with other techniques.

II. ANALYSIS

A. Determination of Appropriate Models

The Widrow-Hopf LMS algorithm for the ALE is as follows [14]:

$$w_{j+1}(k) = w_j(k) + 2\mu \left[x(j)\, x(j - \Delta - k) - x(j - \Delta - k) \cdot \sum_{\ell=0}^{L-1} x(j - \Delta - \ell)\, w_j(\ell) \right], \quad k = 0, 1, \ldots, L - 1 \tag{1}$$

where $w_j(k)$ is the jth update of the kth weight of the ALE; μ is a scalar representing the influence of the input x(j) on the (j + 1)st update of w(k); and L and Δ are, respectively, the number of weights and the delay.

For uncorrelated stationary inputs it has been shown [4, 14, 15] that, starting with an arbitrary initial weight vector, the expected value $w_j(k)$ in (1) converges to the solution of the Wiener-Hopf matrix equation, provided that $0 < \mu < 1/\lambda_{max}$, where λ_{max} is the largest eigenvalue of the data autocorrelation matrix:

$$\lim_{j \to \infty} E[w_j(k)] = w^*(k), \quad k = 0, 1, \ldots, L - 1 \tag{2}$$

[3] Comparisons of various spectral estimation methods, including Fourier and maximum entropy methods (but not adaptive line enhancing), are presented in [12] and [13]. Performance is shown to depend on a number of factors, including the amount of data available and the input signal-to-noise ratio.

where E [·] denotes expectation and w*(k) is the kth component of the L-dimensional vector $\underset{\sim}{W}^*$, which is the solution of the Wiener-Hopf matrix equation:

$$\underset{\sim}{R} \cdot \underset{\sim}{W}^* = \underset{\sim}{P}. \tag{3}$$

In (3) $\underset{\sim}{R}$ is the L × L data autocorrelation matrix with elements $(\underset{\sim}{R})_{\ell k} = \phi_{xx}(\ell - k)$, where $\phi_{xx}(\ell) = E[x(j)\, x(j + \ell)]$ is the autocorrelation function for x(j), and $\underset{\sim}{P}$ is the L-dimensional vector with components $(\underset{\sim}{P})_k = \phi_{xx}(k + \Delta)$.

Further, for the case of uncorrelated input vectors, the covariance of the weight-vector noise in steady state has been shown [1, App. D] to be given by

$$\lim_{j \to \infty} \operatorname{cov} [\underset{\sim}{W}_j - \underset{\sim}{W}^*] = \mu \xi_{min} \underset{\sim}{I} \tag{4}$$

where

$$\xi_{min} = \phi_{xx}(0) - \sum_{k=0}^{L-1} w^*(k)\, \phi_{xx}(k + \Delta) \tag{5}$$

is the minimum mean square error of the finite length Wiener filter $\underset{\sim}{W}^*$ and $\underset{\sim}{I}$ is the L × L identity matrix. The weight vector noise is inherent in the estimation process used in the LMS algorithm and results from performing spectral estimates in a finite observation time. (Note that an exact solution of the Wiener-Hopf matrix equation requires an infinite time history of data, since the exact values of $\phi_{xx}(\ell)$ are required.) The weight vector noise results in an excess steady-state mean-square-error output, so that the ALE error never reaches the theoretical minimum ξ_{min}.

A useful measure of the difference between actual and optimal performance is the "misadjustment," defined as the dimensionless ratio of the average excess mean square error to the minimum mean square error [16]:

$$M = \frac{\text{average excess mean square error}}{\xi_{min}}. \tag{6}$$

The theoretical expression for M derived in [16] is

$$M = \mu L \phi_{xx}(0)\,. \tag{7}$$

Note that (7) was derived under the assumption that the input data are uncorrelated and tends to be smaller than the measured misadjustment when the data are correlated. Note also that the magnitude of the excess error can be made arbitrarily small by making μ arbitrarily small, since a decrease in μ results in an increase in integration time during the adaptive process.

The weight vector noise produces noise in the ALE transfer function. Assuming Gaussian statistics for the weight vector noise, it has been shown [1, App. D] that when the

input noise power in x(j) is large compared to the input signal power, the noise in the transfer function has zero mean and a steady-state power which is given by

$$L\mu\nu^2 \tag{8}$$

where ν^2 is the input noise power. It has also been shown [14, 16] by diagonalizing $\underset{\sim}{R}$ that transients in the mean weight vector consist of sums of exponentials with time constants given by

$$\tau_p \cong \frac{1}{2\mu\lambda_p} \tag{9}$$

where λ_p is the pth eigenvalue of $\underset{\sim}{R}$. In general, a precise treatment of the dynamics of the LMS algorithm is complicated due to the difficulties in diagonalizing $\underset{\sim}{R}$. Note, however, that the dynamics of $E[w_j(k)]$ for the important case of a sinusoid in white noise have been described in [17] by diagonalizing $\underset{\sim}{R}$.

Among the first to consider the convergence of (1) for correlated data was Senne [18], who demonstrated that $E[w_j(k)]$ does not necessarily approach $w^*(k)$ when x(j) is correlated. Further, Senne demonstrated that both the asymptotic excess mean square error and the time constants τ_p increase as correlation increases. Daniell [19] showed that, although the weight vector may be biased away from $\underset{\sim}{W}^*$ in steady state, it can be made arbitrarily close to $\underset{\sim}{W}^*$ in the sense that given any number $\beta > 0$ there exists a $\mu_\beta > 0$ such that for all $0 < \mu < \mu_\beta$

$$\lim_{j\to\infty} \sup E[|\underset{\sim}{W}_j - \underset{\sim}{W}^*|^2] < \beta.$$

The assumptions made by Daniell included ergodicity as well as asymptotic independence and uniform boundedness of the conditional moments of the observable given the past data. As noted by Kim and Davisson [20], this last assumption is rather strong and is not satisfied in a number of important cases. In [20] Kim and Davisson have also considered the convergence properties of adaptive algorithms similar to (1) for correlated stationary input data and were able to show that, under certain assumptions concerning the input data, the mean norm-square of the weight vector deviation converged to asymptotic bounds which can be made arbitrarily small by decreasing the adaptation constant. However, the derivations in [20] require that the adaptive algorithm form its gradient estimate by some averaging of the input data as opposed to using instantaneous data values as in (1). Therefore, the results in [20] do not strictly apply to (1). Other results and references on the convergence properties of (1) for stationary correlated input data are discussed in [17] and [29].

Even though general convergence properties of (1) for stationary correlated input data are very difficult to obtain, it is still reasonable to assume that, for suitably small values of μ, $E[w_j(k)]$ will converge, within a good approximation, to $w^*(k)$ in many cases of practical interest. This assumption, as noted in [1], generally holds in practice, and it will

be used in this paper to derive the expected values of the steady-state ALE weights for stationary inputs consisting of multiple sinusoids in white noise. To verify that the analytical results obtained from the finite length Wiener filter model (3) do in fact describe the steady-state performance of the ALE, experimental results have been obtained using a hardware implementation of the ALE for several special cases. The analytical and experimental results are compared in Section III and are shown to be in good agreement.

B. Steady-State Impulse Response and Transfer Function of the ALE for Multiple Sinusoids in White Noise

Using the Wiener-Hopf model for the ALE response, (3) may be expressed in component form as

$$\sum_{k=0}^{L-1} \phi_{xx}(\ell - k)\, w^*(k) = \phi_{xx}(\ell + \Delta),\ 0 \leqslant \ell \leqslant L-1. \tag{10}$$

When x(j) consists of N sinusoids in white noise,

$$\phi_{xx}(k) = \sigma_0^2\, \delta(k) + \sum_{n=1}^{N} \sigma_n^2 \cos \omega_n k \tag{11}$$

where $\delta(k)$ is the Kronecker delta function (i.e., $\delta(k) = 0$ if $k \neq 0$ and $\delta(0) = 1$). In (11) σ_n^2 is the power in the nth sinusoid, ω_n represents the frequencies of the sinusoids, and σ_0^2 is the white noise power. If $\sigma_0^2 \neq 0$, then $\underset{\sim}{R}$ is positive definite (as shown in the Appendix), and a unique solution to (3) exists.

The inverse of $\underset{\sim}{R}$ can be calculated explicitly, for the special case when $\phi_{xx}(k)$ is given by (11), by the repeated use of a well-known matrix inversion identity sometimes referred to as Woodbury's identity [21]. This identity has been used by a number of authors to analyze $\underset{\sim}{R}^{-1}$ and/or $\underset{\sim}{W}^*$ when $\phi_{xx}(k)$ is in the form of (11). Zeidler and Chabries [3] used this identity to analyze the steady-state properties of the ALE for one sinusoid in white noise, and the use of the identity has been discussed by Lacoss [12], Frost [13], and Marple [30] for purposes of examining different methods of spectral estimation. This inversion identity has also been used by Shapard et al. [22] for purposes of adaptive matrix inversion; by Edelblute et al. [23] to analyze different criteria for optimization of acoustic signal detection; and by Capon [24] to analyze a technique for high resolution frequency-wavenumber spectrum analysis. The application of Woodbury's identity to obtain $\underset{\sim}{W}^*$ is, however, quite tedious and does not resolve many questions concerning the analytic structure of $w^*(k)$ if N is much larger than two.

In this paper it will be shown that solutions for $w^*(k)$ which provide insight into the basic analytic structure of the steady-state ALE impulse response for an arbitrary number of sinusoids can be obtained by an alternate technique called the method of undetermined

coefficients. The method of undetermined coefficients assumes a solution for w*(k) in terms of unknown constants and substitutes this assumed solution into (10) to obtain a set of equations for the unknown constants [25, 26]. Since a unique solution to (10) exists as long as $\sigma_0^2 \neq 0$, a solution to the set of equations for the unknown constants provides the unique solution to (10). It will be shown that for an L-weight filter with N sinusoids present in the input data sequence, the method of undetermined coefficients effectively transforms the set of L coupled equations in (10) into a set of 2N coupled equations. This then leads to a simpler set of equations whenever $L > 2N$. (A procedure similar to this was introduced by Zadeh and Ragazzini [25] for solving the integral equations (analogous to (10)) for the optimum, finite length, continuous predictive filter. This analytical technique was also used by Morgan and Craig [8] to solve (10) for one sinusoid in white noise.)

The form of the assumed solution for w*(k) for N sinusoidal inputs of the form specified in (11) is

$$w^*(k) = \sum_{n=1}^{2N} A_n e^{j\omega_n k} \tag{12}$$

where for notational convenience ω_{n+N} is defined as $-\omega_n (n = 1, 2, \ldots, N)$; the ω_{n+N} are thus the negative frequency components of the input sinusoids. Substituting (12) into (10) with $\phi_{xx}(\ell)$ given by (11), and equating coefficients of $\exp(j\omega_r \ell)$ (for $r = 1, 2, \ldots, 2N$) in the resulting equation, leads to the following 2N equations in the 2N constants A_1, $A_2, \ldots, A_{2N}$:

$$A_r + \sum_{\substack{n=1 \\ n \neq r}}^{2N} \gamma_{rn} A_n = \frac{e^{j\omega_r \Delta}}{L + 2\sigma_0^2/\sigma_r^2}, \quad r = 1, 2, \ldots, 2N \tag{13}$$

where in (13) σ_{n+N}^2 is defined as σ_n^2 $(n = 1, 2, \ldots, N)$ and γ_{rn} is given by

$$\gamma_{rn} = \frac{1}{L + 2\sigma_0^2/\sigma_r^2} \frac{1 - e^{j(\omega_n - \omega_r)L}}{1 - e^{j(\omega_n - \omega_r)}}. \tag{14}$$

The solution of (13) for the A_n completely determines w*(k) through (12).[4] Since N is much smaller than L in many cases of practical interest, (13) often provides a much simpler set of equations than (10).

A number of interesting analytic properties of w*(k) can be observed through (12)–(14). First, (12) implies that when the input to the ALE consists of N sinusoids and additive white noise, the mean steady-state impulse response of the ALE can be expressed as a weighted sum of the positive and negative frequency components of the input sinusoids.

[4] As shown in the Appendix, (13) has a unique solution.

From (14), it is seen that the coefficients γ_{rn}, which couple the A_n together in (13), are proportional to $(1 - e^{j(\omega_n-\omega_r)L})/(1 - e^{j(\omega_n-\omega_r)})$, which is the L-point Fourier transform of exp $(j\omega_n k)$ evaluated at ω_r. Note that from the form of the γ_{rn} it follows that $A_{n+N} = \bar{A}_n$ $(n = 1, 2, \ldots, N)$, where the overbar denotes complex conjugate. This relation is of course necessary to insure that w*(k) is real. A plot of $|\gamma_{rn}|$ versus $\Delta\omega_{nr} \equiv \omega_n - \omega_r$, given in Fig. 2(a) for two different filter lengths and for $2\sigma_0^2/\sigma_r^2 = 1$, shows that, when L is large or when $\Delta\omega_{nr}$ is some integral multiple of $2\pi/L$, γ_{rn} can be neglected. When $\Delta\omega_{nr} \to 0$, $\gamma_{rn} \to (L/2)(\sigma_r^2/\sigma_0^2)/(1 + (L/2)(\sigma_r^2/\sigma_0^2))$; and further, as L becomes large, the ratio of the peaks of $|\gamma_{rn}|$ at $\Delta\omega_{nr} = (2p + 1)\pi/L$ to $|\gamma_{rn}|$ at $\Delta\omega_{nr} = 0$ for $p = 1, 2, \ldots$ is given approximately by $1/(p + 1/2)\pi$. The first two ratios, for instance, are 0.212 and 0.127. Therefore, even if a particular $\Delta\omega_{nr}$ is close to the filter resolution, i.e., within the first several peaks of Fig. 2(a), the associated γ_{rn} could possibly be neglected in (13) without creating serious error in w*(k), especially if $(L/2)(\sigma_r^2/\sigma_0^2)/(1 + (L/2)(\sigma_r^2/\sigma_0^2))$ is much smaller than 1. A specific case when some of the γ_{rn} can be neglected is presented in Section II.C. Note also that as σ_r^2/σ_0^2 becomes very small the γ_{rn} approach zero. This is indicated in Fig. 2(b), where $|\gamma_{rn}|$ is plotted for two different filter lengths and for $2\sigma_0^2/\sigma_r^2 = 50$.

As $\gamma_{rn} \to 0$ for all n and r (i.e., as L becomes large) the A_n uncouple and are given to a good approximation by

$$A_n = \frac{e^{j\omega_n\Delta}}{L + 2\sigma_0^2/\sigma_n^2}, \quad n = 1, \ldots, 2N. \tag{15}$$

Eq. (15) is identical to the expression for the amplitude of the mean steady-state ALE impulse response for one sinusoid at ω_n in white noise previously derived in [1] and [3]. Therefore, as the $\gamma_{rn} \to 0$, the ALE for N sinusoids will adapt to a linear superposition of N independent ALE's, each adapted to a single sinusoid in white noise. From (12), it is seen that the frequency response of the steady-state ALE, which will be denoted by $H^*(\omega)$, can be simply expressed in terms of the A_n:

$$H^*(\omega) \equiv \sum_{k=0}^{L-1} w^*(k)\, e^{-j\omega(k+1)}$$

$$= \sum_{n=1}^{2N} A_n\, e^{-j\omega} \left(\frac{1 - e^{j(\omega_n-\omega)L}}{1 - e^{j(\omega_n-\omega)}} \right). \tag{16}$$

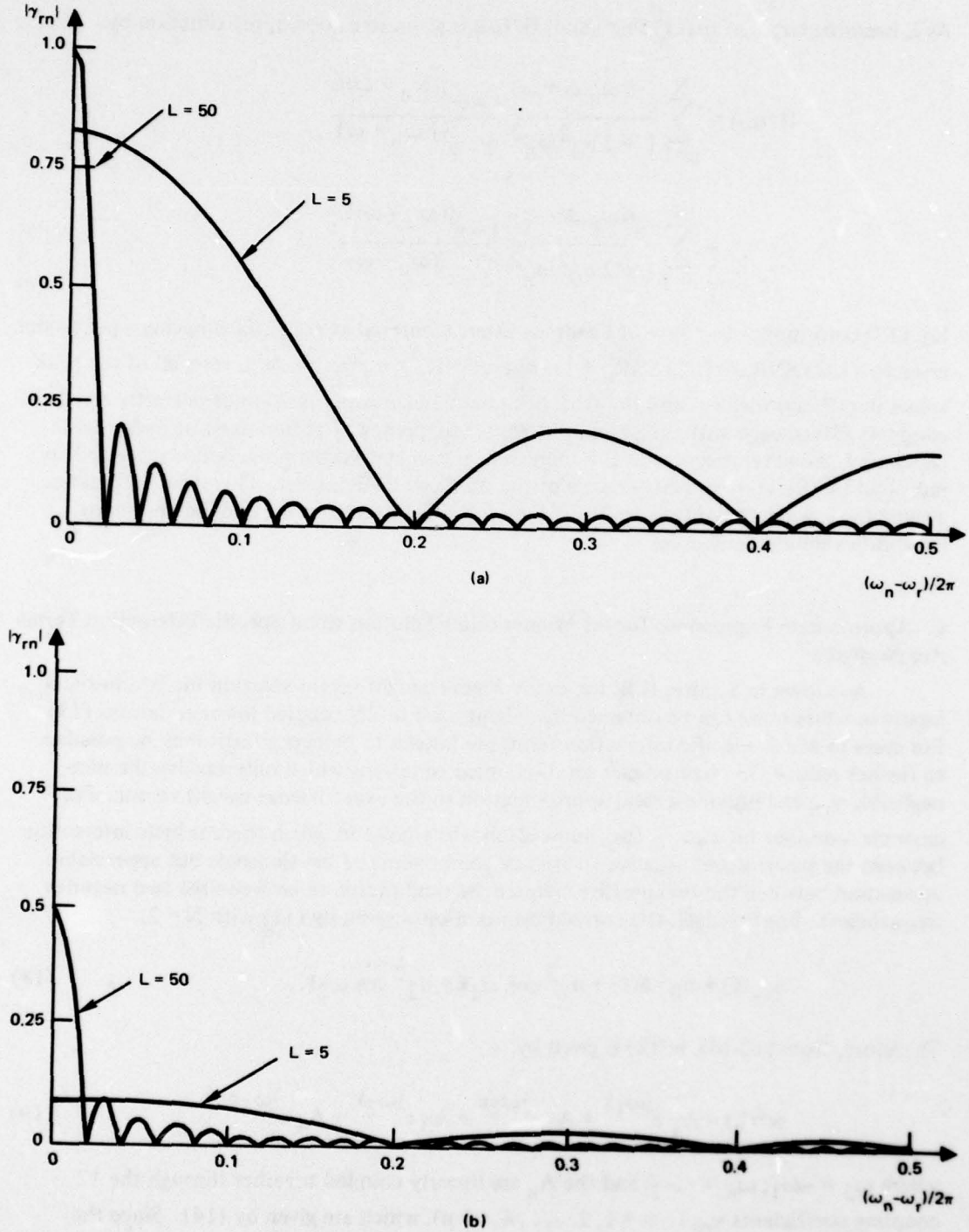

Figure 2. Relation of coupling coefficients γ_{rn} to difference frequencies of simusoidal inputs $\Delta\omega_{nr}$. (a) $2\sigma_0^2/\sigma_r^2 = 1$. (b) $2\sigma_0^2/\sigma_r^2 = 50$.

As L becomes large, so that (15) is valid, $H^*(\omega)$ is given to a good approximation by

$$H^*(\omega) \cong \sum_{n=1}^{N} \frac{e^{-j(\omega_n \Delta + \omega)}}{L + 2\,\sigma_0^2/\sigma_n^2} \frac{1 - e^{-j(\omega_n + \omega)L}}{1 - e^{-j(\omega_n + \omega)}}$$

$$+ \sum_{n=1}^{N} \frac{e^{j(\omega_n \Delta - \omega)}}{L + 2\,\sigma_0^2/\sigma_n^2} \frac{1 - e^{j(\omega_n - \omega)L}}{1 - e^{j(\omega_n - \omega)}} \tag{17}$$

Eq. (17) corresponds to a sum of bandpass filters (centered at $\pm\omega_n$), each having a peak value given by $(L/2)\,SNR_n/((L/2)\,SNR_n + 1)$, where $SNR_n = \sigma_n^2/\sigma_0^2$. As $L \to \infty$, all of the peak values in (17) approach 1, and the ALE becomes a linear superposition of perfectly resolved bandpass filters, each with unit gain at its center frequency. Caution must be exercised in choosing L, however, because as L is increased, the weight vector noise is also increased, as indicated by (8), and the performance of the ALE can be degraded. Therefore, in practice, a value for L which provides a trade-off between weight vector noise and enhancement capabilities should be chosen.

C. Approximate Expressions for the Wiener Filter Solution when Specific Interaction Terms Are Negligible

As shown in Section II.B, the exact Wiener weight vector solution for N sinusoidal inputs in white noise can be obtained by solving a set of 2N coupled linear equations (13). For cases in which specific interaction terms are known to be negligible it may be possible to further reduce (13) to a smaller set of coupled equations which only involve the non-negligible γ_{rn} and provide a valid approximation to the exact Wiener weight vector. For example, consider the case of two sinusoids in white noise in which there is little interaction between the positive and negative frequency components of the sinusoids but appreciable interaction between the two positive frequencies (and therefore between the two negative frequencies). For this case, the correlation function is given by (11) with N = 2.

$$\phi_{xx}(\ell) = \sigma_0^2\,\delta(\ell) + \sigma_1^2 \cos\omega_1\ell + \sigma_2^2 \cos\omega_2\ell. \tag{18}$$

Therefore, from (12-14), $w^*(k)$ is given by

$$w^*(k) = A_1\,e^{j\omega_1 k} + A_2\,e^{j\omega_2 k} + A_3\,e^{j\omega_3 k} + A_4\,e^{j\omega_4 k} \tag{19}$$

where $\omega_3 \equiv -\omega_1$; $\omega_4 \equiv -\omega_2$; and the A_n are linearly coupled together through the 12 coupling coefficients γ_{rn} (r, n = 1, 2, . . . , 4; $r \neq n$), which are given by (14). Since the interaction between the positive and negative frequency components is assumed to be small,

the 8 coefficients $\gamma_{13}, \gamma_{31}, \gamma_{14}, \gamma_{41}, \gamma_{23}, \gamma_{24}, \gamma_{32}, \gamma_{42}$ may be neglected, and (13) reduces to the two independent sets of 2 X 2 linear equations:

$$A_r + \sum_{\substack{n=1 \\ n \neq r}}^{2} \gamma_{rn} A_n = \frac{e^{j\omega_r \Delta}}{L + 2\sigma_0^2/\sigma_r^2}, \quad r = 1, 2 \tag{20}$$

$$A_r + \sum_{\substack{n=3 \\ n \neq r}}^{4} \gamma_{rn} A_n = \frac{e^{j\omega_r \Delta}}{L + 2\sigma_0^2/\sigma_r^2}, \quad r = 3, 4. \tag{21}$$

The solution of (20) and (21) gives the following approximations for the A_n:

$$A_1 = \bar{A}_3 \cong \frac{1}{1 - \gamma_{12}\gamma_{21}} \left[\frac{e^{j\omega_1 \Delta}}{L + 2\sigma_0^2/\sigma_1^2} - \frac{\gamma_{12}\, e^{j\omega_2 \Delta}}{L + 2\sigma_0^2/\sigma_2^2} \right]$$

$$A_2 = \bar{A}_4 \cong \frac{1}{1 - \gamma_{12}\gamma_{21}} \left[\frac{e^{j\omega_2 \Delta}}{L + 2\sigma_0^2/\sigma_2^2} - \frac{\gamma_{21}\, e^{j\omega_1 \Delta}}{L + 2\sigma_0^2/\sigma_1^2} \right] \tag{22}$$

where γ_{12} and γ_{21} are given by (14). As a numerical example illustrating the difference between the approximate solution of (19) – (22) and the exact solution, consider the case when $\omega_1/2\pi = 0.25$; $\omega_2/2\pi = 0.26$; $L = 16$; $\Delta = 5$; and SNR_1 $(= \sigma_1^2/\sigma_0^2) = SNR_2$ $(= \sigma_2^2/\sigma_0^2) = 1.0$. For this case, the magnitudes of the coupling coefficients between the positive and negative frequencies are $|\gamma_{24}| = |\gamma_{42}| = 0.047$; $|\gamma_{23}| = |\gamma_{32}| = |\gamma_{14}| = |\gamma_{41}| = 0.027$; $|\gamma_{13}| = |\gamma_{31}| = 0$. The magnitude of the coupling coefficients between the closely spaced lines is $|\gamma_{12}| = |\gamma_{21}| = |\gamma_{34}| = |\gamma_{43}| = 0.86$. In Fig. 3 plots of $w^*(k)$ derived from (12) – (14) and from the approximations (19) and (22) are presented. As is seen, the greatest discrepancy is approximately 10 percent and occurs at the peaks where the four sinusoids in (19) tend to add constructively.

III. EXPERIMENTAL RESULTS

In this section we apply the analytical results obtained in Section II for N sinusoids in uncorrelated noise to the specific cases of a single sinusoid in white noise and two sinusoids in white noise. Experimental verification that the steady-state response of the ALE is in fact described by the Wiener filter model for these cases is provided. The experimental date presented in this paper were obtained on a variable length hardware implementation of

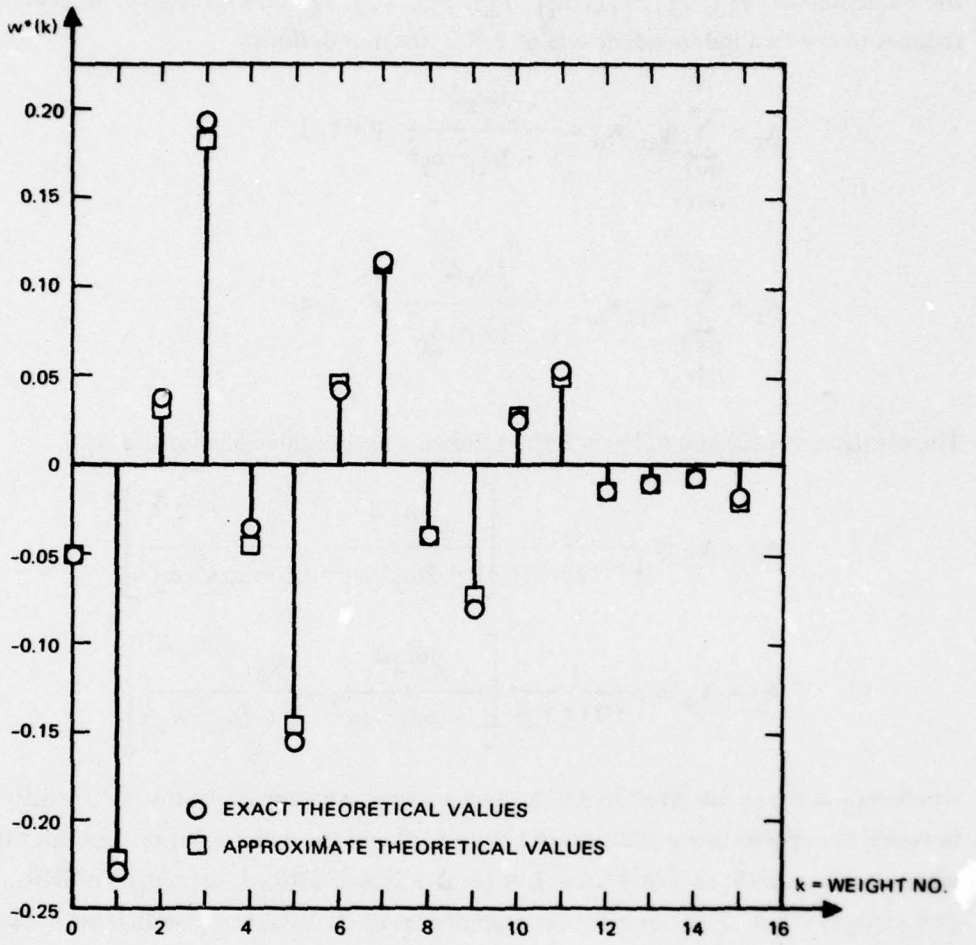

Figure 3. Comparison of weight values derived from (12)–(14) and from approximations (19) and (22) for a particular case defined in the text.

the ALE which employed 9-bit linear quantization in the upper (input) channel and 4-bit log quantization in the adaptive filter (reference) channel of Fig. 1. Filter lengths of 8, 16, 32, 64, 128, and 256 weights can be obtained with this hardware. Experimental plots of the frequency response of the ALE in steady state were obtained by "freezing" the weights at a particular instant (after adaptation), and applying white noise to the input of the stationary filter and spectral-analyzing the resulting output. The value of $\mu\phi_{XX}(0)$ used in the experiments was sufficiently small that weight vector noise was negligible. The noise spectrum was obtained from a thermal noise generator whose output was filtered by a –48-dB per octave low-pass filter with its –3-dB point at 1.8 kHz. The input noise spectrum was thus only approximately flat in the region of interest. The major sources of experimental error were the low-pass characteristics of the input noise spectrum and quantization noise. Input levels

for all experiments were controlled to insure that the error due to quantization noise was approximately 2 percent. All the experimental curves presented in this section were obtained directly from x-y pen plots of the spectrum analyzer output. All the theoretical curves were obtained by evaluating the quantity of interest at 10 X L different frequency values between $\omega = 0$ and $\omega = \pi$. The input sampling rate was 3.9 kHz in all cases.

A. One Sinusoid in White Noise

For this case the correlation function $\phi_{xx}(\ell)$ is given by

$$\phi_{xx}(\ell) = \sigma_0^2\, \delta(\ell) + \sigma_1^2 \cos \omega_1 \ell. \tag{23}$$

Therefore, from (12)–(14), $w^*(k)$ is given by

$$w^*(k) = A_1\, e^{j\omega_1 k} + A_2\, e^{-j\omega_1 k} \tag{24}$$

where

$$A_1 = \bar{A}_2 = \frac{1}{L + 2\sigma_0^2/\sigma_1^2}\, \frac{1}{1 - |\gamma_{12}|^2}\, [e^{j\omega_1 \Delta} - \gamma_{12}\, e^{-j\omega_1 \Delta}] \tag{25}$$

and

$$\gamma_{12} = \frac{1}{L + 2\sigma_0^2/\sigma_1^2}\, \frac{1 - e^{-2j\omega_1 L}}{1 - e^{-2j\omega_1}}. \tag{26}$$

In this particular case, γ_{12} represents coupling between the positive and negative frequency components of the real sinusoid. Note that as $\gamma_{12} \to 0$, i.e., as the frequency components become uncoupled, $w^*(k)$ is given to a good approximation by

$$w^*(k) \cong \frac{SNR}{1 + SNR(L/2)} \cos \omega_1 (k + \Delta) \tag{27}$$

with $SNR \equiv \sigma_1^2/\sigma_0^2$. Therefore, as long as there is negligible coupling between the positive and negative frequency components of the sinusoid, the steady-state impulse response of the ALE is a sampled cosinusoid at frequency ω_1 which has been shifted in phase by $\omega_1 \Delta$. The amplitude of the cosinusoid is SNR/(1 + SNR(L/2)). This result was also obtained in [3] and discussed in [1, App. D]. However, as γ_{12} becomes appreciable, the amplitude and phase shift of the steady-state ALE impulse response begin to change considerably, as is observed in (24) – (26).

Fig. 4 represents the results of an experiment carried out on a 16-weight ALE with $\Delta = 8$ samples, $\mu\phi_{xx}(0) = 5.12 \times 10^{-6}$, and an input sinusoid with SNR $\equiv \sigma_1^2/\sigma_0^2 = 0.557$ and frequency $\omega_1/2\pi = 0.0039$.[5] For this frequency there is appreciable coupling between the positive and negative frequency components of the sinusoid. Experimental plots of the input and ALE output power spectrum (plotted on the same relative log scale and denoted by $S_x(\omega)$ and $S_y(\omega)$, respectively) are presented in Fig. 4(a). In Fig. 4(b) three curves are presented. The first two curves are experimental and theoretical linear plots of $|H^*(\omega)|$ and the third is a linear plot of the function

$$|G(\omega)| \equiv \frac{1}{L + 2\sigma_0^2/\sigma_1^2} \left| e^{-j\omega_1\Delta} \left\{ \frac{1 - e^{-j(\omega_1 + \omega)L}}{1 - e^{-j(\omega_1 + \omega)}} \right\} + e^{j\omega_1\Delta} \left\{ \frac{1 - e^{j(\omega_1 - \omega)L}}{1 - e^{j(\omega_1 - \omega)}} \right\} \right| \tag{28}$$

where $\Delta = 8$. The term $|G(\omega)|$ in (28) is the Fourier transform of $w^*(k)$ with $\gamma_{12} = 0$. This curve is included to show the effects of the coupling coefficient γ_{12} on the frequency response of the steady-state ALE. As is seen, the effect of the coupling coefficient is to reduce the peak values and null depths in $|H^*(\omega)|$. Neglecting the coefficient when $\omega_1 << 2\pi/L$ can give rise to serious errors, as is observed in Fig. 4(b). It should be noted that there is excellent agreement between the theoretical and experimental curves of $|H^*(\omega)|$ with respect to the location of the peaks and nulls. There is some discrepancy in the two curves, however, with respect to the amplitudes of $|H^*(\omega)|$, especially in the higher frequency ranges. This discrepancy is mainly due to the nonflatness of the noise spectrum used to generate the experimental curve. As a further means of comparing the experimental ALE steady-state weight vector and the Wiener weight vector, the misadjustment M defined by (6) was determined with measured values of the steady-state ALE mean square error output. For the case represented by Fig. 4, M was found to be approximately 1 percent. The theoretical misadjustment, calculated with (7), which includes gradient estimation noise only, was approximately 0.01 percent for this case. (In these experiments gradient estimation noise was a negligible source of error compared to quantization noise and other factors.)

In Fig. 5 experimental and theoretical plots of 20 log $|H^*(\omega_1)|$ are presented for different input SNR. These data were obtained from an 8-weight ALE with $\Delta = 199$ samples and $\omega_1/2\pi = 0.098$. Note that the two curves agree within the experimental error of the measurements. (The bars in Fig. 5 denote the estimated variances of the measurements.)

---

[5] In this section all frequencies have been normalized to the sample frequency; arrows in the figures denote the actual location of the input sinusoids.

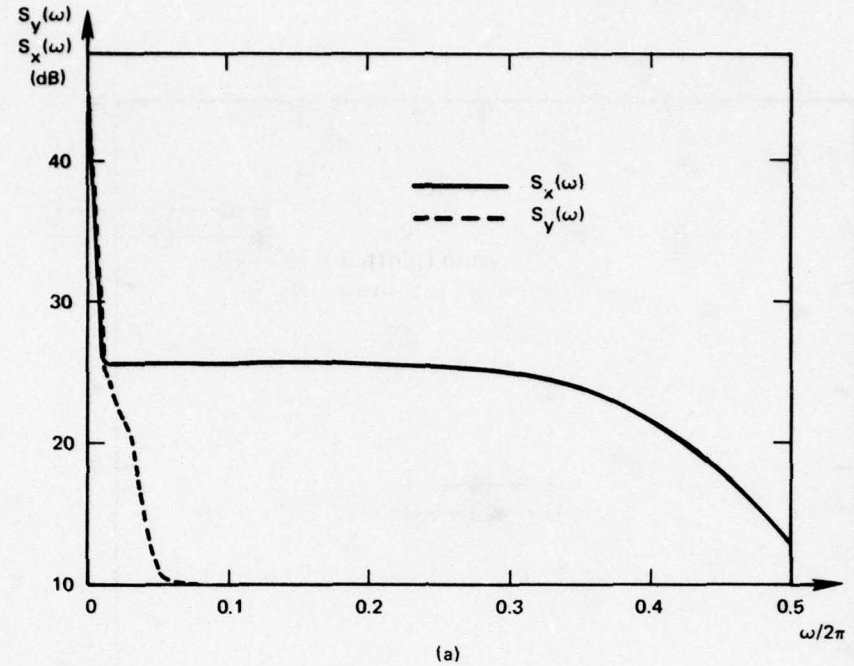

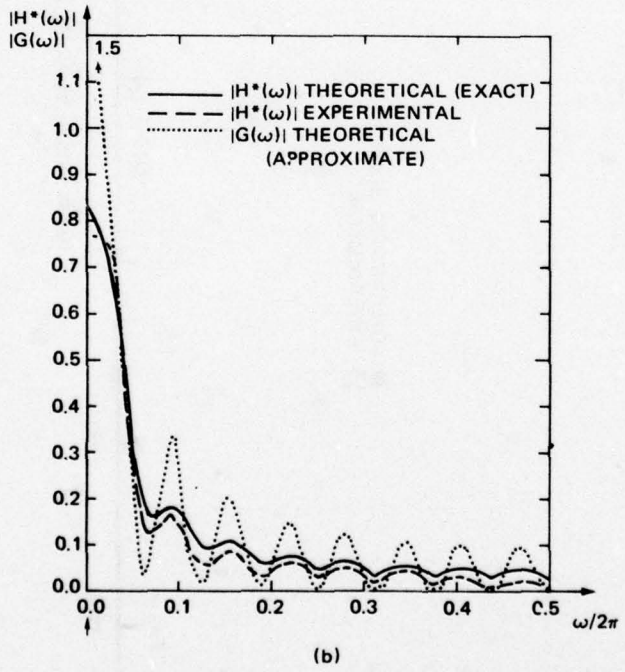

Figure 4. Performance of 16-weight ALE with input of single sinusoid in uncorrelated noise; delay $\Delta = 8$ samples; $\mu\phi_{xx}(0) = 5.12 \times 10^{-6}$; input signal-to-noise ratio SNR = 0.557. (a) Power spectra of input $S_x(\omega)$ and steady-state output $S_y(\omega)$. (b) Experimental and theoretical steady-state transfer function $|H^*(\omega)|$ and $|G(\omega)|$ defined in text.

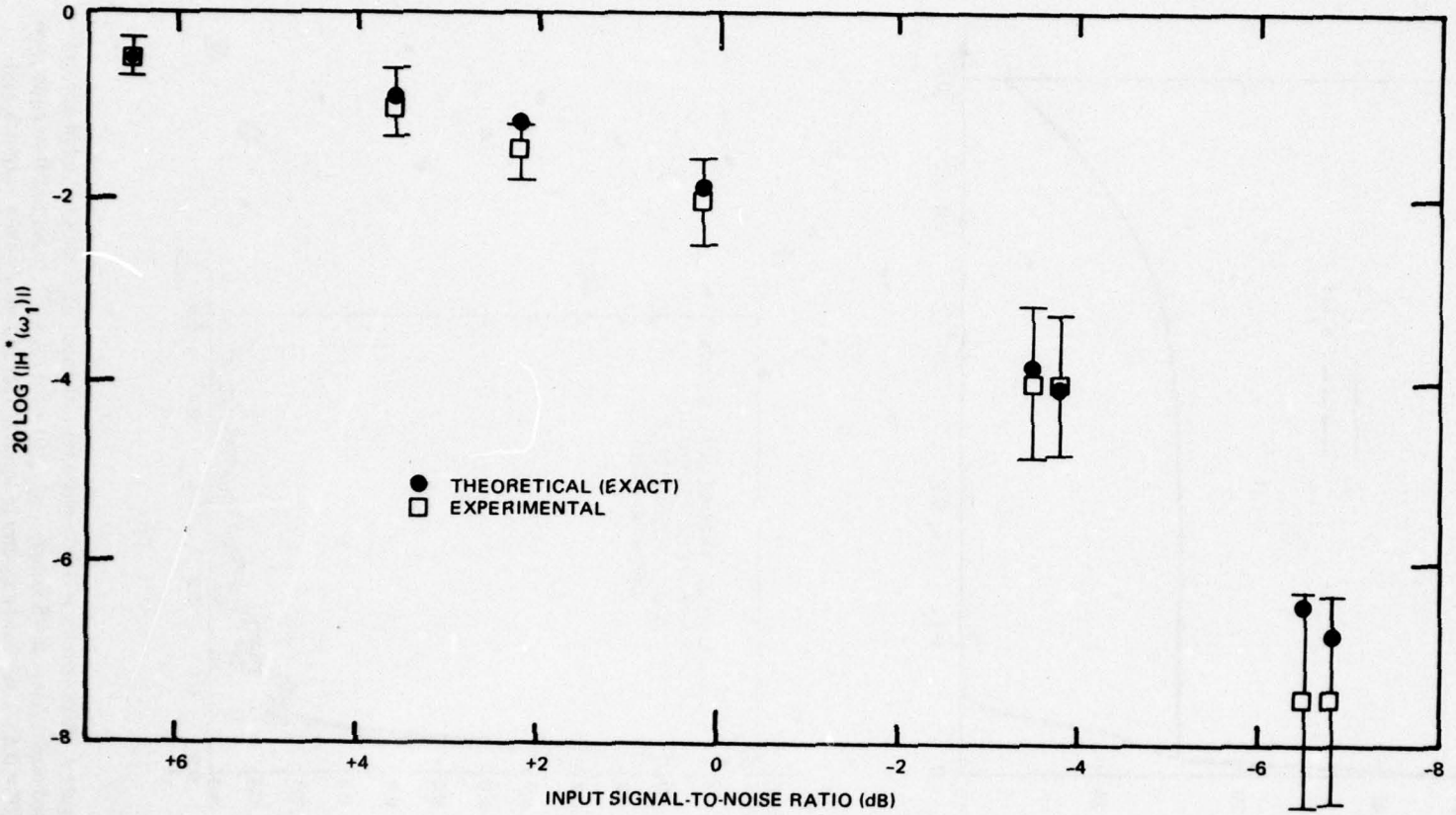

Figure 5. Experimental and theoretical plots of 20 log ($|H^*(\omega_1)|$) for an 8-weight ALE as a function of input signal-to-noise ratio for single sinusoid in uncorrelated noise.

B. Two Sinusoids in White Noise

For the case of two sinusoids in white noise the autocorrelation function of the input is as given by (18). The expected value of the steady-state ALE impulse response can be expressed as a sum of sinusoids as in (19), where the amplitudes of the sinusoids A_n are the solution of (13).

Figs. 6–8 represent the results of three experiments carried out on a 32-weight ALE which illustrate the effect of the variable prediction distance Δ on the impulse response and transfer function of a finite length linear predictive filter. In these experiments the frequencies of the sinusoids were $\omega_1/2\pi = 0.0768$ and $\omega_2/2\pi = 0.09984$. In Figs. 6 and 7, $\sigma_1^2/\sigma_0^2 = \sigma_2^2/\sigma_0^2 = 1$; in Fig. 8, $\sigma_1^2/\sigma_0^2 = 1$ and $\sigma_2^2/\sigma_0^2 = 0.36$. Experimental plots of the ALE input and output power spectrum (in dB) for these cases are presented in Figs. 6(a), 7(a), and 8(a). Figs. 6(b) and 8(b) compare the experimentally measured transfer function of the ALE with the analytical results obtained for $\Delta = 6$ samples, $L = 32$, and the frequencies and SNR's of the two sinusoids defined above. Figs. 7(b) and 7(c) compare the experimentally measured impulse response and transfer function of the ALE with theory for the case where $\Delta = 19$ samples and all other parameters are identical to those chosen in Fig. 6. As shown in Figs. 6(b) and 8(b), when $\Delta = 6$ samples there is a deep null in $|H^*(\omega)|$ at $\omega \cong (\omega_1 + \omega_2)/2 \equiv \omega_{av}$; whereas, when $\Delta = 19$ samples (Fig. 7(c)), the null is practically gone. The null at $\Delta = 6$ samples and the two highest peaks in the transfer function in Figs. 6(b) and 8(b) occur in spite of the fact that the frequency resolution of the filter is too coarse to resolve the two input sinusoids. It should be noted that the phase difference between the sinusoidal components of $w^*(k)$ in (19) has shifted the locations of the two highest peaks in $|H^*(\omega)|$ away from the frequencies of the input sinusoids, as indicated in Figs. 6(b) and 8(b).

For the case of two sinusoids which are separated in frequency by $\Delta\omega \equiv \omega_2 - \omega_1$, the delay which is required to produce the null effect shown in Figs. 6 and 8 will become larger as $\Delta\omega \to 0$. To verify this, note that $|H^*(\omega_{av})|$ for the two sinusoids in Figs. 6–8 is given to a good approximation by

$$|H^*(\omega_{av})| \cong \left| A_1 \frac{1 - e^{-j\Delta\omega L/2}}{1 - e^{-j\Delta\omega/2}} + A_2 \frac{1 - e^{j\Delta\omega L/2}}{1 - e^{j\Delta\omega/2}} \right| . \tag{29}$$

In (29) we have neglected the effects of the negative frequency components of the sinusoids (which is a good approximation for the parameters in Figs. 6–8). Under this assumption, A_1 and A_2 are given by (22). Eq. (29) can then be expressed in the following form:

$$|H^*(\omega_{av})| = F\sqrt{a^2 + b^2 + 2ab \cos \Delta\omega((L-1)/2 + \Delta)} \tag{30}$$

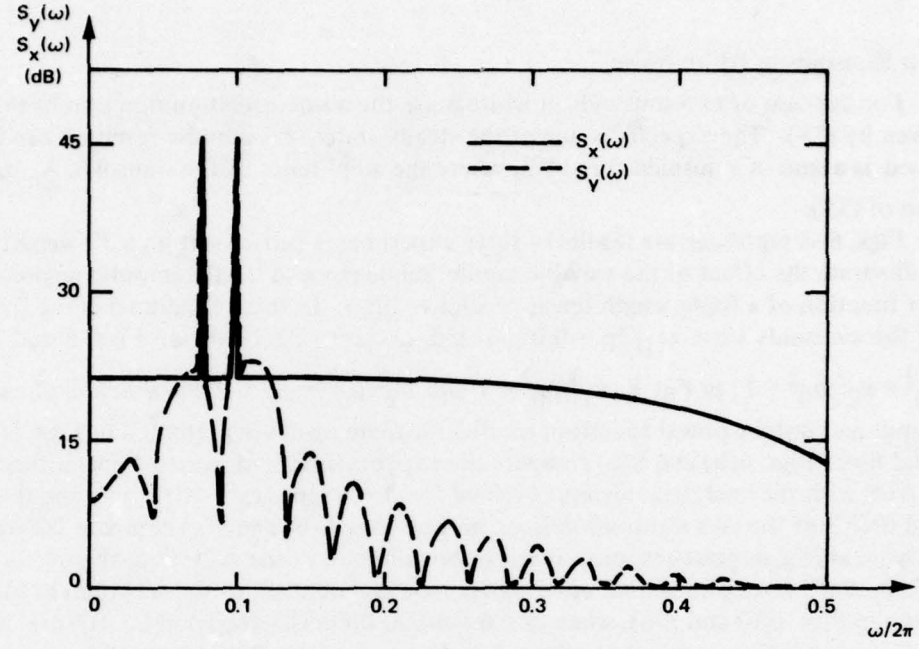

(a)

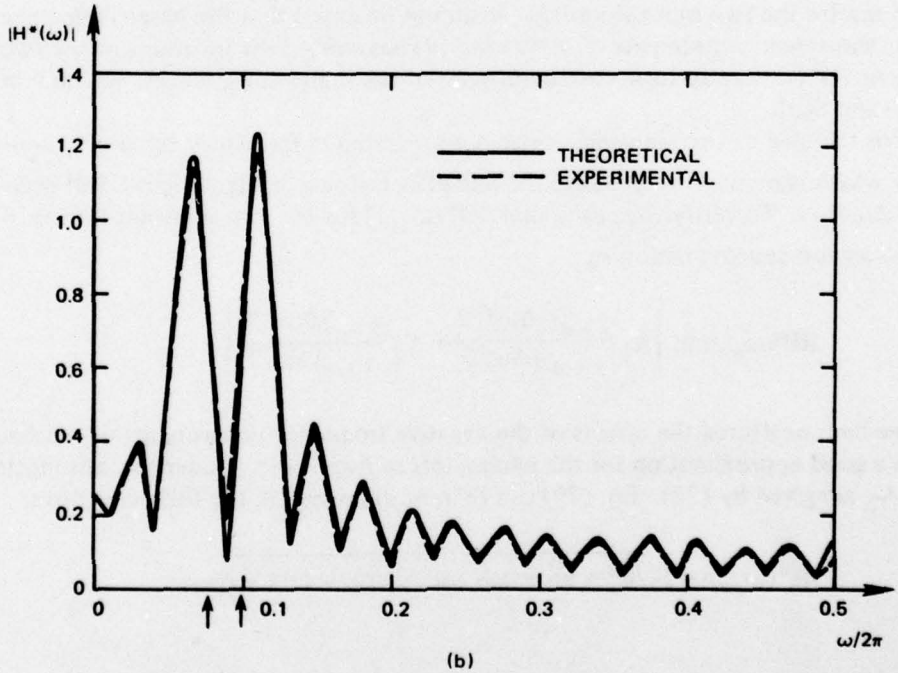

(b)

Figure 6. Performance of 32-weight ALE with input of two sinusoids of equal power in uncorrelated noise; delay $\Delta = 6$ samples; $\mu\phi_{xx}(0) = 3.6 \times 10^{-6}$. (a) Power spectra of input $S_x(\omega)$ and steady-state output $S_y(\omega)$. (b) Experimental and theoretical steady-state transfer function $|H^*(\omega)|$.

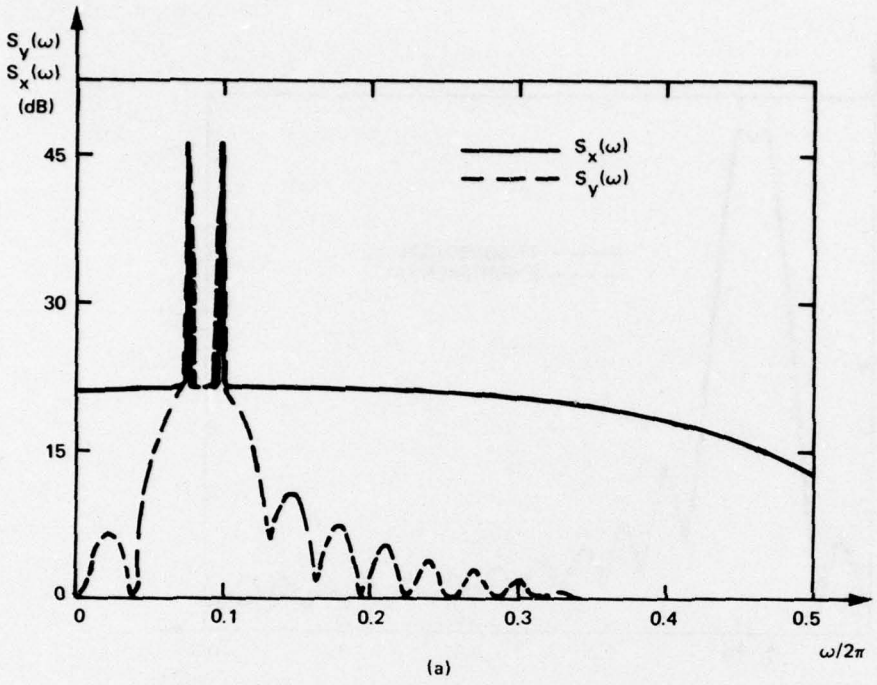

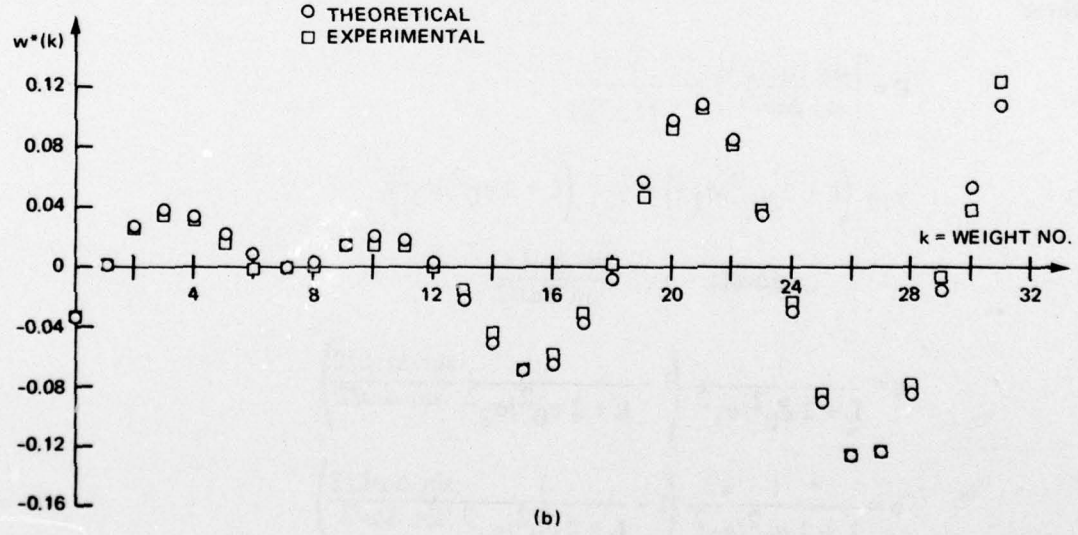

Figure 7. Performance of 32-weight ALE with input of two sinusoids of equal power in uncorrelated noise; delay $\Delta = 19$ samples; $\mu\phi_{xx}(0) = 3.6 \times 10^{-6}$. (a) Power spectra of input $S_x(\omega)$ and steady-state output $S_y(\omega)$. (b) Experimental and theoretical steady-state impulse response $w^*(k)$.

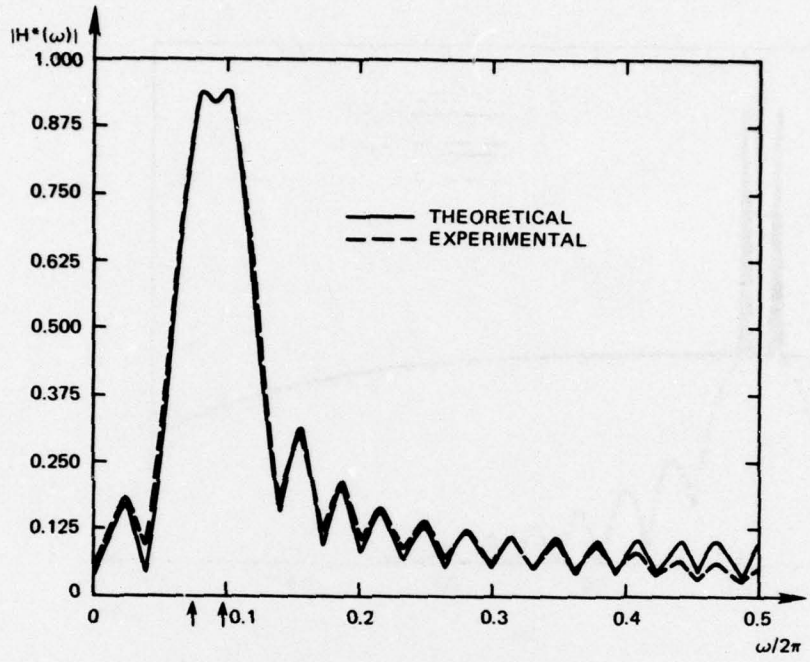

Figure 7. (Continued.) (c) Experimental and theoretical steady-state transfer function $|H^*(\omega)|$.

where

$$F = \left| \frac{\sin \Delta\omega L/4}{\sin \Delta\omega/4} \right| \frac{1}{1 - \gamma_{12}\gamma_{21}}$$

$$\gamma_{12}\left(L + 2\sigma_0^2/\sigma_1^2\right) = \bar{\gamma}_{21}\left(L + 2\sigma_0^2/\sigma_2^2\right)$$

$$= e^{j\Delta\omega(L-1)/2} \frac{\sin \Delta\omega L/2}{\sin \Delta\omega/2}$$

$$a = \frac{1}{L + 2\sigma_0^2/\sigma_1^2}\left(1 - \frac{1}{L + 2\sigma_0^2/\sigma_2^2} \frac{\sin \Delta\omega L/2}{\sin \Delta\omega/2}\right)$$

$$b = \frac{1}{L + 2\sigma_0^2/\sigma_2^2}\left(1 - \frac{1}{L + 2\sigma_0^2/\sigma_1^2} \frac{\sin \Delta\omega L/2}{\sin \Delta\omega/2}\right).$$

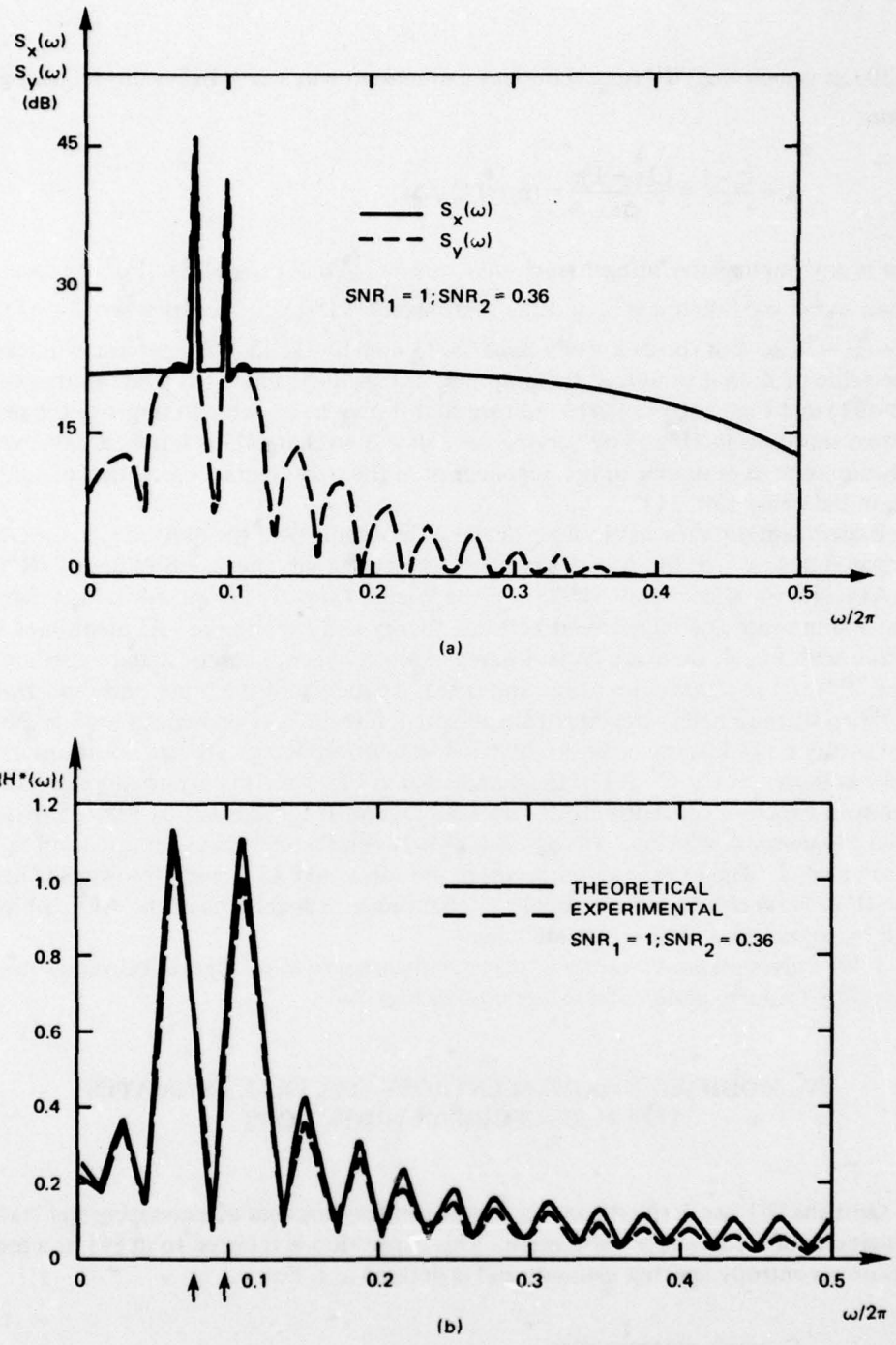

Figure 8. Performance of 32-weight ALE with input of two sinusoids of unequal power in uncorrelated noise; delay $\Delta = 6$ samples, $\mu\phi_{xx}(0) = 2.83 \times 10^{-6}$. (a) Power spectra of input $S_x(\omega)$ and steady-state output $S_y(\omega)$. (b) Experimental and theoretical steady-state transfer function $|H^*(\omega)|$.

From (30), it is seen that $|H^*(\omega_{av})|$ obtains a minimum when Δ satisfies the following condition:

$$\Delta + \frac{L-1}{2} = \frac{(2n+1)\pi}{\Delta\omega} = (n + 1/2)/\Delta f \tag{31}$$

where n is any nonnegative integer (such that $(n + 1/2)/\Delta f > (L - 1)/2$). For the special case when $\sigma_1^2 \cong \sigma_2^2$, then $a \cong b$, and the first zero of $|H^*(\omega_{av})|$ occurs when $\Delta = (1/2)(1/\Delta f) - (L - 1)/2$. For the case when $\Delta f = 0.023$ and $L = 32$, $\Delta \cong 6$ samples, which agrees with the value of Δ that produced the deep null in Figs. 6(b) and 8(b). The results expressed by (29)–(31) and Figs. 6(b) and 8(b) indicate that it may be possible to improve the resolution of two sinusoids in $H^*(\omega)$ by varying the delay Δ so that (31) is satisfied. This variation of resolution with Δ is similar to the dependence of the periodogram resolution of sinusoids on their initial phase [30, 31].

Experimentally measured values of the ALE weights and the derived values of $w^*(k)$ are compared in Fig. 7(b) for $\Delta = 19$ samples. Experimentally measured values of $|H^*(\omega)|$ for the ALE and the theoretical $|H^*(\omega)|$ of the Wiener filter are compared in Figs. 6(b), 7(c), and 8(b) and indicate good agreement between theory and experiment. As mentioned in connection with Fig. 4, there are larger discrepancies between theoretical and experimental values of $|H^*(\omega)|$ at frequencies nearer the cutoff frequency of the input noise spectrum.

When the number of weights of the adaptive filter is large enough to resolve the frequencies of the sinusoids, the peaks in $|H^*(\omega)|$ will correspond to the true locations of the sinusoids, as shown in Fig. 9. All of the parameters in Fig. 9 are in correspondence with the parameters in Figs. 6–7, except that $\Delta = 15$ samples and L is increased to 128 to provide improved frequency resolution. The agreement between theory and experiment in Fig. 9(b) is seen to be good. The experimental curves of the input and ALE output power spectra for this case (Fig. 9(a)) clearly indicate the line enhancement capabilities of the ALE, which are achieved by suppressing the uncorrelated noise.

Table I gives measured values of misadjustment, as well as theoretical values from (7), corresponding to the experimental values used in Figs. 6–9.

IV. MODIFIED MAXIMUM ENTROPY SPECTRAL ESTIMATES FOR N SINUSOIDS IN WHITE NOISE

Griffiths [4] has defined a useful expression for purposes of estimating and tracking the frequencies of sinusoids in white noise. This expression is referred to in [4] as a modified maximum entropy spectral estimate and is defined as follows:

$$Q_x(\omega) = \frac{1}{|1 - H^*(\omega)|^2} \tag{32}$$

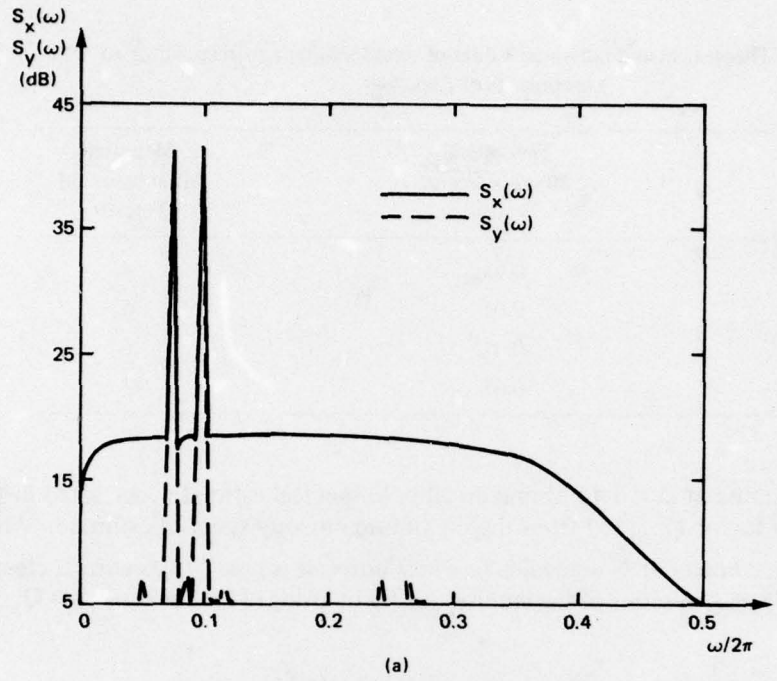

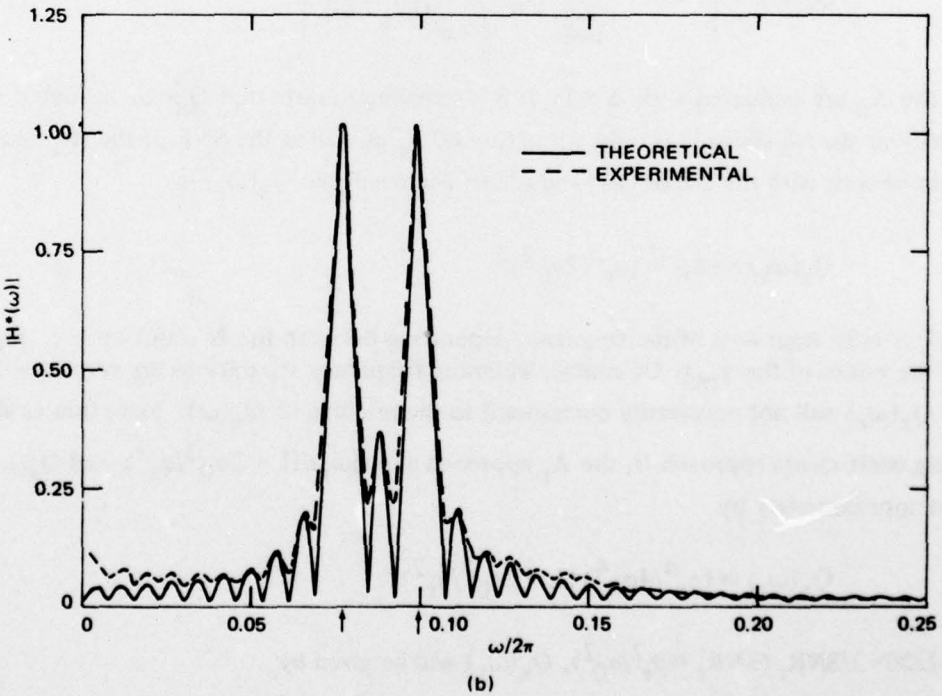

Figure 9. Performance of 128-weight ALE with input of two sinusoids of equal power in uncorrelated noise; delay $\Delta = 15$ samples, $\mu\phi_{xx}(0) = 3.6 \times 10^{-6}$. (a) Power spectra of input $S_x(\omega)$ and steady-state output $S_y(\omega)$. (b) Experimental and theoretical steady-state transfer function $|H^*(\omega)|$.

Table I. Theoretical and measured values of misadjustment corresponding to experiments of Figs. 6–9.

Experiment	Theoretical Misadjustment, Percent	Measured Misadjustment, Percent
Fig. 6	0.01	4
Fig. 7	0.01	5
Fig. 8	0.01	6
Fig. 9	0.05	3

where $H^*(\omega)$ is evaluated at $\Delta = 1$ to obtain an all-pole spectral estimate. As noted in [4], $Q_x(\omega)$ differs by the factor ξ_{min} (5) from the maximum entropy spectral estimate. When the input to the ALE consists of N sinusoids in white noise, it is possible to write a closed form expression for $Q_x(\omega)$ in terms of the amplitudes A_n by using (12). The result for $Q_x(\omega)$ is

$$Q_x(\omega) = \left| 1 - e^{-j\omega} \sum_{n=1}^{2N} A_n \frac{1 - e^{j(\omega_n - \omega)L}}{1 - e^{j(\omega_n - \omega)}} \right|^{-2} \tag{33}$$

where the A_n are evaluated with $\Delta = 1$. It is interesting to note that $Q_x(\omega)$ evaluated at the frequency of the rth sinusoid is only a function of A_r as well as the SNR of the rth sinusoid. This can be seen with the use of (13) and (33). The result for $Q_x(\omega_r)$ is

$$Q_x(\omega_r) = |A_r|^{-2} (\sigma_r^2/2\sigma_0^2)^2. \tag{34}$$

Eq. (34) is valid regardless of the frequency separation between the N sinusoids (i.e., regardless of the values of the γ_{rn}). Of course, when the frequency separations are very small, the values $Q_x(\omega_r)$ will not necessarily correspond to the maxima of $Q_x(\omega)$. Note that as all the coupling coefficients approach 0, the A_r approach $\exp(j\omega_r)/(L + 2\sigma_0^2/\sigma_r^2)$, and $Q_x(\omega_r)$ is given approximately by

$$Q_x(\omega_r) \cong (\sigma_r^4/4\sigma_0^4)(L + 2\sigma_0^2/\sigma_r^2)^2 . \tag{35}$$

When $L >> 2/SNR_r$ ($SNR_r = \sigma_r^2/\sigma_0^2$), $Q_x(\omega_r)$ will be given by

$$Q_x(\omega_r) \cong \frac{SNR_r^2}{4} L^2 . \tag{36}$$

Eq. (34) shows that the value $Q_x(\omega_r)$ is, in effect, influenced by all of the other sinusoids at $\omega = \omega_n$ $(n \neq r)$ through coupling terms γ_{rn}. Eqs. (35)–(36) show that, as these terms approach zero, $Q_x(\omega_r)$ becomes independent of all the other sinusoids and depends only on the SNR of the rth sinusoid. Similar results have also been obtained by Lacoss [12] for the theoretical peak values of the maximum entropy estimate of one sinusoid in white noise using Woodbury's identity. A further discussion of these theoretical results as well as similar results corresponding to sinusoids in one-pole low-pass noise is given in [32].

For the purpose of comparing $Q_x(\omega)$ and $H^*(\omega)$, plots of the modified maximum entropy spectral estimate $Q_x(\omega)$ defined by (32) are presented in Fig. 10 corresponding to the frequencies, SNR's, and filter length of Figs. 6–8. The plots of $Q_x(\omega)$ in Fig. 10 were calculated from the theoretical values of $H^*(\omega)$ computed from the Fourier transform of the $w^*(k)$ given by (12).[6] It is seen in Figs. 10(a) and 10(b) that, in contrast to the plots of $|H^*(\omega)|$ in Figs. 6(b), 7(c), and 8(b), the theoretical estimate $Q_x(\omega)$ gives the frequency location of the sinusoids more accurately.

It should be noted that Griffiths [4] has shown that the instantaneous adaptive estimate $\hat{Q}_x(\omega; j)$, which is defined as in (32), with $H^*(\omega)$ replaced by

$$\sum_{k=0}^{L-1} w_j(k)\, e^{-j\omega(k+1)}$$

where $w_j(k)$ is obtained from (1) with $\Delta = 1$, provides a good frequency estimate of sinusoids in white noise, especially for high input SNR cases. The theoretical plots of $Q_x(\omega)$ in Fig. 10 indicate that even when the input SNR's are not very large, $\hat{Q}_x(\omega; j)$ may still provide a very good frequency estimate of the input signals. However, as the input noise is increased, the variance in the ALE weight vector noise increases (for μ fixed), and the confidence in $\hat{Q}_x(\omega; j)$ as a spectral estimate will be degraded to some extent. Baggeroer [27], in deriving confidence intervals for maximum entropy (MEM) spectral estimates, has considered the relevant case of several closely spaced sinusoids in white noise. For this case, Baggeroer has shown that although the MEM has very large peak-to-background ratios, the confidence intervals associated with these peaks can be quite large. In deriving the MEM confidence intervals, Baggeroer assumed that the MEM estimate is formed by segmenting the input data sequence into constant length data blocks. Although this particular method of segmenting the data into blocks is used in most direct, or FFT, methods of spectral estimation, it is not the method which is used to form the adaptive MEM spectral estimate $\hat{Q}_x(\omega; j)$. In contrast to segmenting the input data, the ALE (as noted in [10]) works on a steady flow of data that it weights exponentially over time. Therefore, unresolved questions arise with respect to the confidence (especially at the peaks) of the adaptive MEM spectral estimate. Of course, the confidence

[6] Corresponding experimental plots of $Q_x(\omega)$ were not available from the particular hardware implementation of the ALE used in the experiments.

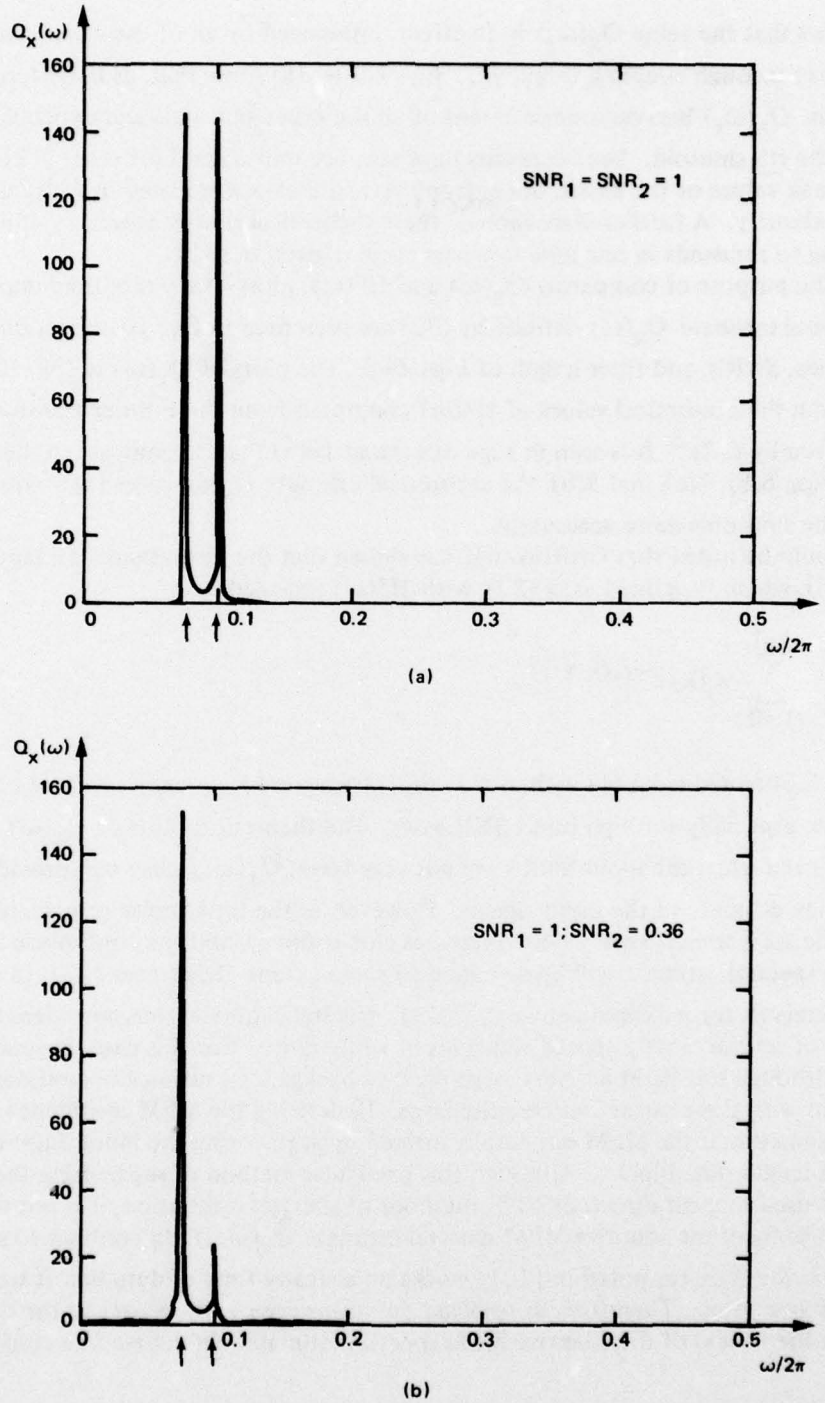

Figure 10. Theoretical performance of 32-weight ALE implemented as a maximum entropy frequency tracker with delay $\Delta=1$. (a) With input of two sinusoids of equal power in uncorrelated noise. (b) With input of two sinusoids of unequal power in uncorrelated noise.

intervals for $\hat{Q}_x(\omega;j)$ can be reduced by decreasing μ; however, this will also increase the ALE data processing time. Therefore, the usefulness of $\hat{Q}_x(\omega;j)$ for purposes of real-time spectral estimation in noisy environments is not yet understood.

V. CONCLUSIONS

The steady-state behavior of the ALE has been analyzed in this paper for stationary inputs consisting of multiple sinusoids in white noise using constrained Wiener filter theory. An analytic solution for an L-weight discrete Wiener filter has been derived for N sinusoids in white noise. This solution shows that the expected values of the ALE weights in steady state can be written as a sum of sinusoids and that the amplitude of each sinusoid A_n ($n = 1, 2, \ldots, 2N$) is coupled to the amplitude of all the other sinusoids by coefficients which approach zero as the ALE filter length becomes large. This particular representation for the steady-state weights is equivalent to a transformation of the $L \times L$ Wiener-Hopf matrix equation to a set of 2N coupled linear equations for the amplitudes A_n. When $N \geq 2$, the transformation method becomes much simpler to use than Woodbury's identity (which has been used considerably by a number of authors to examine maximum entropy filtering of sinusoids in white noise; see e.g. [12], [13] and [30]). Comparisons between the theoretical expressions derived in Section II and experimentally measured impulse responses and transfer functions of the steady-state ALE (obtained from an ALE hardware implementation) for one and two sinusoidal inputs in white noise were presented in Section III and indicate the validity of the analytical models used in Section II. The modified maximum entropy spectral estimate $Q_x(\omega)$ was also analyzed in Section IV for multiple sinusoidal inputs in white noise. Since the analytical results presented in this paper were obtained on the basis of constrained Wiener filter theory for a finite length linear prediction filter with arbitrary prediction distance, they describe the performance of a much wider class of linear predictive filters than the specific implementation known as the ALE.

Extensions of the analytical results given in this paper to more general types of rational input spectra are currently being carried out and will be presented in a future paper. It has been shown that the method of undetermined coefficients also provides useful analytical solutions of the discrete Wiener-Hopf matrix equation (3) for general rational input spectra [28].

APPENDIX

The purpose of this appendix is twofold. First, it will be shown that $\underline{R}$ is positive when $\phi_{xx}(k)$ is given by (11) with $\sigma_0^2 \neq 0$. Second, it will be shown that (13) has a unique solution when $\sigma_0^2 \neq 0$. The proof of the first statement is trivial and consists of examining

the quadratic form of $\underset{\sim}{R}$. Let $\underset{\sim}{x}$ be a nonzero L-dimensional column vector and denote by $\underset{\sim}{x}^T$ the transpose of $\underset{\sim}{x}$. Then the quadratic form of $\underset{\sim}{R}$ using the notation of (12)–(13), is given as

$$\underset{\sim}{x}^T \underset{\sim}{R} \underset{\sim}{x} = \sigma_0^2 \sum_{r=0}^{L-1} |x_r|^2 + 1/2 \sum_{k=1}^{2N} \sigma_k^2 \sum_{r=0}^{L-1} \sum_{n=0}^{L-1} x_r e^{j\omega_k(r-n)} x_n$$

$$= \sigma_0^2 \sum_{r=0}^{L-1} |x_r|^2 + 1/2 \sum_{k=1}^{2N} \sigma_k^2 \left| \sum_{r=0}^{L-1} x_r e^{-j\omega_k r} \right|^2 \qquad \text{(A.1)}$$

However, the last expression for $\underset{\sim}{x}^T \underset{\sim}{R} \underset{\sim}{x}$ in (A.1) is strictly positive for nonzero x, and therefore $\underset{\sim}{R}$ is positive definite.

To see that (13) has a unique solution when $\sigma_0^2 \neq 0$, note that it may be expressed in the equivalent form (by multiplying the rth equation of (13) by $L + 2\sigma_0^2/\sigma_r^2$):

$$\underset{\sim}{B} \cdot \underset{\sim}{A} = \underset{\sim}{C} \qquad \text{(A.2)}$$

where $\underset{\sim}{B}$ is a 2N × 2N Hermitian matrix with elements

$$(\underset{\sim}{B})_{rn} = (2\sigma_0^2/\sigma_r^2)\,\delta(r-n) + \sum_{k=0}^{L-1} e^{-j(\omega_r - \omega_n)k};$$

$\underset{\sim}{A}$ is a 2N-dimensional column vector with components $(\underset{\sim}{A})_n = A_n$; and $\underset{\sim}{C}$ is a 2N-dimensional column vector with components $(\underset{\sim}{C})_r = \exp(j\omega_r\Delta)$. To show that (A.2) has a unique solution we will show that $\underset{\sim}{B}$ is positive definite. Let $\underset{\sim}{x}$ be a nonzero 2N-dimensional column vector and $\underset{\sim}{x}^H$ be its complex conjugate transpose. Then, the quadratic form of $\underset{\sim}{B}$ is written as

$$\underset{\sim}{x}^H \underset{\sim}{B} \underset{\sim}{x} = \sum_{r=1}^{2N} |x_r|^2 (2\sigma_0^2/\sigma_r^2) + \sum_{r=1}^{2N} \sum_{n=1}^{2N} \bar{x}_r \sum_{k=0}^{L-1} e^{-j(\omega_r - \omega_n)k} x_n$$

$$= \sum_{r=1}^{2N} |x_r|^2 (2\sigma_0^2/\sigma_r^2) + \sum_{k=0}^{L-1} \left| \sum_{r=1}^{2N} x_r e^{j\omega_r k} \right|^2 . \qquad \text{(A.3)}$$

As observed in connection with (A.1), the last expression for $\underset{\sim}{x}^H \underset{\sim}{B} \underset{\sim}{x}$ in (A.3) is strictly positive for nonzero $\underset{\sim}{x}$, and therefore $\underset{\sim}{B}$ is positive definite.

REFERENCES

1. B. Widrow, J. Glover, J. McCool et al., "Adaptive noise cancelling: Principles and applications," Proc. IEEE, vol. 63, pp. 1692-1716, Dec. 1975.

2. J. McCool and B. Widrow, "Principles and applications of adaptive filters: A tutorial review," Naval Undersea Center, San Diego, Calif., Technical Publication 530, March 1977; also presented at the IEE International Specialist Seminar on the Impact of New Technologies in Signal Processing, Aviemore, Scotland, Sept. 1976.

3. J. Zeidler and D. Chabries, "An analysis of the LMS adaptive filter used as a spectral line enhancer," Naval Undersea Center, San Diego, Calif., Technical Publication 556, February 1975.

4. L. Griffiths, "Rapid measurement of digital instantaneous frequency," IEEE Trans. Acous., Speech, and Sig. Proc., vol. ASSP-23, pp. 209-222, April 1975.

5. R. Keeler and L. Griffiths, "Acoustic Doppler extraction by adaptive linear prediction filtering," J. Acous. Soc. Amer., vol. 61, pp. 1218-1227, May 1977.

6. T. Kailath, "A view of three decades of linear filtering theory," IEEE Trans. Inform. Theory, vol. IT-20, pp. 145-181, March 1974.

7. J. Makhoul, "Linear prediction: A tutorial review," Proc. IEEE, vol. 63, pp. 561-580, April 1975.

8. D. Morgan and S. Craig, "Real-time linear prediction using the least mean square gradient algorithm," IEEE Trans. Acous., Speech, and Sig. Proc., vol. ASSP-24, pp. 494-507, Dec. 1976.

9. D. W. Tufts, "Adaptive line enhancement and spectrum analysis," Proc. IEEE (letters), vol. 65, pp. 169-170, Jan. 1977.

10. B. Widrow, J. Glover, J. McCool, and J. Treichler, Reply to letter from D. W. Tufts, Proc. IEEE (letters), vol. 65, pp. 171-173, Jan. 1977.

11. L. Griffiths, Reply to letter from D. W. Tufts, Proc. IEEE (letters), vol. 65, pp. 170-171, Jan. 1977.

12. R. Lacoss, "Data adaptive spectral analysis methods," Geophysics, vol. 36, pp. 661-675, Aug. 1971.

13. O. Frost, "Power spectrum estimation," in Aspects of Signal Processing with Emphasis on Underwater Acoustics, Part 1, G. Tacconi, Ed. Boston: D. Reidel Pub. Co., 1977, pp. 125-162.

14. B. Widrow, "Adaptive filters," in Aspects of Network and System Theory, R. Kalman and N. DeClaris, Eds. New York: Holt, Rinehart, and Winston, 1971, pp. 563-587.

15. B. Widrow, P. Mantey. L. Griffiths, and B. Goode, "Adaptive antenna systems," Proc. IEEE, vol. 55, pp. 2143-2159, Dec. 1967.

16. B. Widrow, J. McCool, M. Larimore, and C. Johnson, Jr., "Stationary and nonstationary learning characteristics of the LMS adaptive filter," Proc. IEEE, vol. 64, pp. 1151-1162, Aug. 1976.

17. J. Treichler, "The spectral line enhancer," Ph.D. Dissertation, Dept. of Electrical Engineering, Stanford Univ., Stanford, Calif., May 1977.

18. K. Senne, "Adaptive linear discrete-time estimation," Stanford Electronics Lab., Stanford Univ., Stanford, Calif., Rep. SEL-68-090, June 1968 (Ph.D. Dissertation).

19. T. Daniell, "Adaptive estimation with mutually correlated training samples," IEEE Trans. Systems Science and Cybernetics, vol. SSC-6, pp. 12-19, Jan. 1970.

20. J. Kim and L. Davisson, "Adaptive linear estimation for stationary M-dependent processes," IEEE Trans. Inform. Theory, vol. IT-21, pp. 23-31, Jan. 1975.

21. G. Zielke, "Inversion of modified symmetric matrices," J. Assoc. Comp. Machinery, vol. 15, pp. 402-408, 1968.

22. J. Shapard, D. Edelblute, and G. Kinnison, "Adaptive matrix inversion," Naval Undersea Center, San Diego, Calif., Technical Note 528, May 1971.

23. D. Edelblute, J. Fisk, and G. Kinnison, "Criteria for optimum-signal-detection theory for arrays," J. Acous. Soc. Amer., vol. 41, pp. 199-205, Jan. 1967.

24. J. Capon, "High-resolution frequency-wavenumber spectrum analysis," Proc. IEEE, vol. 57, pp. 1408-1418.

25. L. Zadeh and J. Ragazzini, "An extension of Wiener's theory of prediction, J. Appl. Phys., vol. 21, pp. 645-655, July 1950.

26. L. Zadeh and J. Ragazzini, "Optimal filters for the detection of signals in noise," Proc. IRE, vol. 40, p. 1223, 1952.

27. A. Baggeroer, "Confidence intervals for regression (MEM) spectral estimates," IEEE Trans. Inform. Theory, vol. IT-22, pp. 534-545, Sept. 1976.

28. E. Satorius and J. Zeidler, "Least-mean-square, finite length, predictive digital filters," Conference Record of the IEEE International Conference on Acoustics, Speech, and Signal Processing, Hartford, Conn., May 9-11, 1977.

29. J. Kaunitz, "Adaptive filtering of broadband signals as applied to noise cancelling," Stanford Electronics Lab., Stanford Univ., Stanford, Calif., Rep. SEL-72-038, Aug. 1972 (Ph.D. Dissertation).

30. S. Marple, "Conventional Fourier, autoregressive, and special ARMA methods of spectrum analysis," Engineer thesis, Dept. of Electrical Engineering, Stanford Univ., Stanford, Calif., 1976.

31. P. Jackson, "Truncations and phase relationships of sinusoids," J. Geoph. Research, vol. 72, pp. 1400-1403, Feb. 1967.

32. E. Satorius and J. Zeidler, "Maximum entropy spectral analysis of multiple sinusoids in noise," Geophysics (forthcoming).